ISSN: 2278-0181
NCERAME - 2015 Conference Proceedings

Experimental Investigation of Static Pressure Distribution on the Flat Surface Due to Impingement of Air Jets

Ritesh. B. Dhamoji [1], Harish Kumar [2], Raju. B. S [3] , Manjunatha L H[4]
[1]PG Student, School of Mechanical Engineering, REVA University, Bangalore.
[2] Assistant Professor, School of Mechanical Engineering, Reva University
[3] Associate professor, school of Mechanical engineering, Reva University
[4] Professor & Head, Mechanical Engineering, REVA ITM/RU

Abstract:- **The promising technique of impingement cooling of such components needs primary attention as this technique is associated with non-uniform distribution of heat transfer coefficients. The designer sand researchers may choose suitable impingement cooling system based on the permissible non-uniformities of heat transfer rates depending on scheme of application. The present work is to address the issue of non-uniformity. This may be accomplished by obtaining the local heat transfer and fluid flow distributions due to various schemes of jet impingement cooling and there by quantify its degree of non-uniformity.**
Hence, present work aims to investigate the local heat transfer and fluid flow characteristics due to impingement on flat surface which simulates leading edge of a typical gas-turbine blade. Further it is aimed to investigate separately the influence of geometric parameters of jets and target surface on local distribution of heat transfer coefficients and wall static pressure distribution. Thin foil and Infrared radiometry technique used by Lytle and Webb [27] will be considered in the present study of local temperature measurement. The uncertainty analysis will be carried out for all the parameter estimation as detailed by Moffat

Key words: Air jets, Static Pressure distribution, Venturimeter

1. INTRODUTION

The jet impingement heat transfer is one of the well-established high performance techniques for heating, cooling and drying of a surface. Such impinging flow devices allow for short flow paths on the surface with relatively high heat transfer rates .Interest and researching this topic continues unabated and may have even accelerated in recent years because of its high potential of local heat transfer enhancements. Applications of the impinging jets include drying of textile sand film; cooling of gas turbine components and the outer wall of combustors; and cooling of electronic equipment.
Single jet finds its application mostly where highly localized heating or cooling is necessary. However, when large surface areas require cooling or heating, multiple jet impingements are desirable. The proposed research work is to focus study on gas turbine blade cooling application which requires multiple jet-impingements.

The efficiency of the gas-turbine engines depend primarily on the turbine in let gas temperatures. The metallurgical considerations of the gas-turbine blade put a limit on the maximum in let gas temperature. Hence, an option to improve the engine efficiency could be to device an effective method to cool the turbine blades. A promising method of cooling turbine blades is to impinge cool air on the internal surfaces of the blades so that the gas turbine cycle may be operated at higher engine compression ratios with higher inlet gas temperatures for higher efficiencies and reduced fuel consumption. VanTreuren [1] reports a reduction of blade metal temperature of 40°*C* can improve blade life tenfold. Han*etal*.[2] reports that turbine entry temperatures in some of the advanced gas turbines are far higher than the melting point of the blade material hence, the turbine blades need to be efficiently cooled using the relatively cool air bled from the compressor for improved performance.

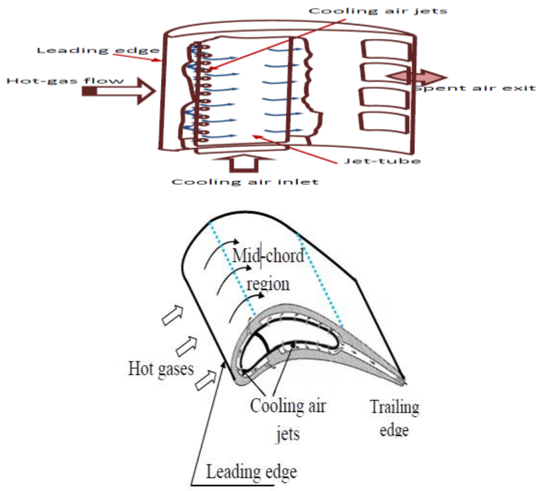

Fig.1: cooling of gas turbine blade with a row of impinging jets

Hence, this region needs primary attention of efficient cooling method. The internal passage at the leading edge may be considered to have a semi-circular concave surface and this region may be convectively cooled by a span wise row of impinging jets. In order to design and choose an effective cooling method, the knowledge of the local heat transfer characteristics and wall static pressure distribution of the blade are essential.

2. LITERATURE REVIEW

The high heat transfer rates associated with impinging air jet is well recognized and documented for many years. Review of the experimental work on impinging jets is reported by Living ood and Hrycak [3], Martin [4], Jambunathan*etal.*[5] and Viskanta[6].

The available literature reveals that there have been some experimental investigations on flow and heat transfer characteristics of semi-circular concave surface with arrow of impinging jets which typically simulate cooling of leading edge of gas turbine blades. One of the first investigations on the impingement of a row of circular jets on a concave surface is reported by Chupp*etal.*[7].Their configuration simulated cooling internal passages of leading edge of typical gas-turbine blade. Jusionis [8], Metzger*etal.*[9,10] and Dyban and Mazur[11] have studied the influence of Reynolds number(*Re*)and other geometric parameters on the average heat transfer characteristics in a semi-circular concave surface impinged by single row of circular jets. Taslimet *al.* [12-15], Taslimand Khanicheh[16] and Taslimand Bethka[17] made extensive experimental and numerical investigate on off low and heat transfer due to impingement on a smooth and rib-roughened leading-wall of gas turbine for constant *z/d* and *s/d* at different Reynolds number. Their study included average heat transfer characteristics for different flow conditions. They reported that the air mass flow rate through all the holes remains almost same for the cases of flow entering the supply channel from one end or both ends. Iacovides*etal.*[18],studied experimentally the flow and thermal development of a row of cooling jets impinging on a rotating concave surface. Cooling fluid is injected from a row of five jet holes along the center line of the flat surface of the passage and strikes the concave surface. Craft*etal* [19] studied modeling of three-dimensional jet array impingement and heat transfer on a concave surface. Fenot*etal.*[20] carried out experimental investigation of heat transfer due to arrow of air jets impinging on a concave semi-cylindrical surface. The jets are issued from round tubes and flow to the supply channel is normal to the concave surface. However most of the heat transfer studies are not well supported by the wall static pressure measurements on the cylindrical concave surface along both the longitudinal and circumferential directions .Tabakoff and Clevenger[21] studied the effect of surface curvature on wall static pressure distribution for slot jet impingement .They varied the ratio of diameter of flat surface to slot width between 5.0 and 20.0 at constant jet-to-surface distance of six times jet width. They found that, the wall static pressure decrease along the curvature at higher rate at lower ratios of diameter of flat surface to slot width. Florschuetz*et al*.[22]studied flow distribution characteristics for arrays of impinging jets on flat surface. They developed a theoretical model to predict the row-by-row flow distribution and compared their results with the experiments. Choi*etal*[23] carried out LD A measurement of mean and fluctuating components of velocity in an experimental study with converging slot jet impinging on a concave surface. Recently, Ramakumarand Prasad [24, 25] reported experimental and computational results of the flow characteristics from multiple circular air jets impinging on a concave surface. They reported experimental results for the configuration of D/d=30,s/d=5.4andz/d=1.0.However,their study does not explicitly correlate the influence of jet-to-plate distance on wall static pressure at a given Reynolds number. Bunker[26] reports about many and mostly unattended major thermal issues of turbine cooling as advanced engine design has allowed surpassing normal material temperature limits. One of the key issues includes uniformity of internal cooling of turbine blade passages.

3. CONCLUSIONS FROM LITERATURE SURVEY AND OBJECTIVE OF PRESENT PROPOSED WORK:

The promising technique of impingement cooling of such components needs primary attention as this technique is associated with non-uniform distribution of heat transfer coefficients. The designer sand researchers may choose suitable impingement cooling system based on the permissible non-uniformities of heat transfer rates depending on scheme of application. The present work is to address the issue of non-uniformity. This may be accomplished by obtaining the local heat transfer and fluid flow distributions due to various schemes of jet impingement cooling and there by quantify its degree of non-uniformity.

Hence, present work aims to investigate the local heat transfer and fluid flow characteristics due to impingement on flat surface which simulates leading edge of a typical gas-turbine blade. Further it is aimed to investigate separately the influence of geometric parameters of jets and target surface on local distribution of heat transfer coefficients and wall static pressure distribution. Thin foil and Infrared radiometry technique used by Lytle and Webb [27] will be considered in the present study of local temperature measurement. The uncertainty analysis will be carried out for all the parameter estimation as detailed by Moffat [28].

4. OBJECTIVES OF THE PRESENT WORK

Based on the literature review the following objectives are defined for the present work. The present work is to study experimentally the distribution of static pressure on the flat surface due to air jet impingement from long pipe circular nozzle.

- Study the influence of Reynolds number of flow on the static pressure distribution on the flat surface. The experiment is conducted for the

Reynolds number of flow ranging from 12000 to 47000.

- Study the influence of longitudinal distance(X) on the static pressure distribution on the flat surface for various Reynolds number of flow and distance between target plate and nozzle (Z).

- Study the influence of longitudinal distance from point of impingement of jet (X) on the static pressure distribution on the flat surface for various Reynolds number of flow and distance between target plate and nozzle (Z).

- Study the influence of distance between target plate and nozzle (Z) on the static pressure distribution on the flat surface for different Reynolds number and along transverse axis(Z)

5. DESIGN OF VENTURIMETER

Discharge through a pipe is usually measured by providing co-axial area contraction within the pipe and by recording the pressure drop across the contraction.

A venturimeter is a device consisting of a short length of gradual convergence and a longer length of gradual divergence. Semi angle of convergence is 8^0 to 10^0 and the semi angle of convergence is 3^0 to 5^0. A pressure tapping is provided at a location before the convergence commences and another pressure tapping is provided at the throat section of the venturimeter. The pressure difference (p_1-p_2) between the two tappings is measured by means of a U tube manometer. The manometer may contain water or mercury as manometric fluid depending upon the pressure difference is expected. A flow nozzle is a device in which the contraction of area is brought by nozzle. One of the pressure tappings is provided at a distance of one diameter upstream the nozzle plate and other at the nozzle exit.

Air blower AEG GM 600E (600W, 6 Speed, 0-16000rpm)

- Minimum pressure rise at lower speed of blower = 4mm of Hg
- Maximum pressure rise at maximum speed of blower=33mm of Hg
- **Density of air at 35⁰C (ρ_a)**

$$\rho_a=\frac{P}{RT}=\frac{101.325*10^3}{0.287*308}=\mathbf{1.146}\ \mathbf{Kg/m^3} \ \ldots\ldots\textbf{eq. (1)}$$

- **Pressure head (h_a)**

$$h_a=\frac{\rho_m*h_m}{\rho_a}=\frac{13.6*10^3*4*10^{-3}}{1.146}=47.47\ \ldots\ldots\text{eq.(2)}$$

- **Velocity of air through Orifice (V_o)**

$$V_o=C_d\sqrt{2*g*ha} = 0.62\sqrt{2*9.81*47.47} = \mathbf{18.92}\ m/s$$
….eq. (3)

- **Flow rate (Q_o)**

A_o= Area of orifice, d_0 = Diameter of orifice.

$$A_o=\frac{\pi}{4}*d_0^2=\frac{\pi}{4}*(20*10^{-3})^2=\mathbf{3.14*10^{-4}m^2} \ \textbf{...eq. (4)}$$

$$Q_o= A_oV_o = 3.14*10^{-4}*18.92=\mathbf{0.356\,m^3/min}$$

Consider,

Minimum flow rate Qmin= **0.36** $\mathbf{m^3}/\boldsymbol{min}$

Maximum flow rate $\mathbf{Q_{max}}$ = **2.8** $\mathbf{m^3}/\boldsymbol{min}$ (Rated by Manf.)

5.1. THROAT DIAMETER

Throat diameter is designed to get minimum **50mm** deflection in water manometer for Q_{min}

Flow through Venturimeter is given by

$$Q_v=\frac{a_1*a_2}{\sqrt{a_1^2-a_2^2}}\sqrt{2*g*ha}\ \ldots\ldots\ldots\text{eq. (5)}$$

For 50mm deflection of water at 35℃

h_a= 43.63 m of air

$$\frac{0.36}{60}=\frac{5.1*10^{-4}*a_2}{\sqrt{(5.1*10^{-4})^2-a_2^2}}\sqrt{2*9.81*43.63}$$

$a_2 = 1.90*10^{-4}\ m^2$

$d_2^2=\frac{4}{\pi}*a_2=\frac{4}{\pi}*1.90*10^{-4}$

$d_2 = 0.01556$ m = 15.56 mm

Considering d_2= 16mm

Inlet diameter d_1 = 25.4mm

Throat diameter d_2= 16mm

5.2. Length of manometer:

For maximum flow rate length of manometer is

$$\frac{2.8}{60}=\frac{5.1*10^{-4}*2.01*10^{-4}}{\sqrt{(5.1*10^{-4})^2-(2.01*10^{-4})^2}}\sqrt{2*9.81*ha}\ \ldots\ldots\text{eq. (6)}$$

h_a= 2321 m of air

$$h_w=\frac{h_a*\rho_a}{\rho_w}=\frac{2321*1.146}{1000}=2.65\text{ m of water}$$

5.3. Design of venturimeter:

For convergent angle $\theta_1 = 10^0$

$$\tan\theta_1=\frac{d_1-d_2}{2*l_1}=\frac{25.4-16}{2*l_1}\ \ldots\ldots\text{eq.(7)}$$

l_1 = 26.65 mm ≈ 27 mm

For divergent angle $\theta_2 = 5^0$

$$\tan\theta_2=\frac{d_1-d_2}{2*l_2}=\frac{25.4-16}{2*l_2}$$

l_2 = 53.721 mm ≈ 54 mm

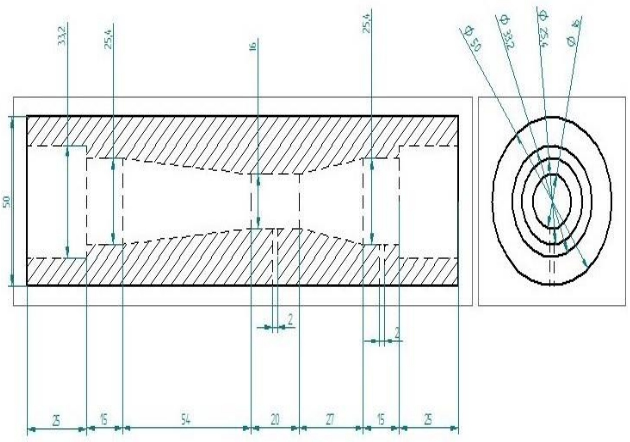

Fig.5.1: 2-D Venturimeter

Venturimeter Dimensions:

Inlet Diameter: d_1= 25.4 mm

Throat Diameter: d2= 16 mm

Convergent Angle: $\Theta_1=10^0$

Divergent Angle: $\Theta2=5^0$

5.4. *Calibration of venturimeter*

Venturimeter is a device used to measure flow rates. The basic principle on which venturiemeter works is that by reducing the cross-sectional area of the passage, a pressure difference is created and measurement of pressure difference ensures the discharge through the pipe. Since the cross-sectional area of throat is smaller than the cross-sectional area of the inlet section, because of which the velocity of flow at throat become greater than at the inlet section. The increase in velocity of flow at throat resists decrease in pressure at this section. The pressure difference between these two sections is determined by connecting a differential manometer between the taps provided at these sections; measurement of pressure difference enables the rate of flow to be calculated.

The actual discharge (Q_{act}) is calculated by

$$Q_{act}=\frac{A*h}{t}$$

If"Ao"and"A2"be the cross-sectional areas of the inlet and throat sections respectively and "H"is the difference between pressure head sand "g" acceleration due to gravity then the theoretical discharge (Q_{th}) is given by

$$Q_{th}=\frac{a_1*a_2}{\sqrt{a_1{}^2-a_2{}^2}}\sqrt{2*g*(\frac{\rho_w}{\rho_a}-1)*ha}\text{........eq. (8)}$$

The co-efficient of discharge is given by

$$C_d=\frac{Q_{act}}{Q_{the}}\text{ ....eq. (9)}$$

The diameter of the inlet and outlet are measured and their cross-sectional area is calculated. A differential manometer is connected at the inlet and throat sections and water is allowed to pass through the venturiemeter. The dimensions of the collecting tank are noted, the difference between the two limbs of the manometer are noted. The flow is then varied and above procedure is repeated for different Reynolds number, Reynolds numbers are varied from 10000-100000 trials for particular Reynolds number is done and the results are tabulated. Actual and theoretical values of discharge are calculated, and co-efficient of discharge determined by the ratio of actual /theoretical discharge values.

Fig. 5.2: venturiemeter

Calculations:

Blower: - AEG GM 600E

Minimum volume flow rate of air for given air blower

Q_{min}= 0.36 m^3/min

Minimum mass flow rate:

$$m_{min}=\frac{0.36*1.1425}{60}=6.88*10^{-3}\text{ kg/s}$$

Maximum volume flow rate of air for given air blower:

Q_{max}= 2.8 m^3/min

Maximum mass flow rate:

$$m_{max}=\frac{2.8*1.1425}{60}=0.053316\text{ kg/s}$$

Reynolds number for minimum flow rate of air

$$Re_{min}=\frac{\rho*V*d1}{\mu}=\frac{4*m_{min}}{\pi*d1*\mu}=\frac{4*6.88*10^{-3}}{\pi*0.0254*1.983*10^{-5}}=16846.94\text{ ....eq. (10)}$$

Reynolds number for maximum flow rate of air

$$Re_{max}=\frac{4*m_{max}}{\pi*d1*\mu}=\frac{4*0.053316}{\pi*0.0254*1.983*10^{-5}}=134775.59\text{......eq. (11)}$$

Venturimeter calibration with water at average temperature 30^0c

μ_w= 8.315*10^{-4} kg/m-s

$$R_e=\frac{\rho*V*d1}{\mu_w}=\frac{4*m_w}{\pi*d1*\mu_w}$$

$$R_e=\frac{4*\left[\frac{a_1*a_2}{\sqrt{a_1^2-a_2^2}}*\sqrt{2*g*h_w}\right]*\rho_w}{\pi*d1*\mu_w}=\frac{4*\left[\frac{a_1*a_2}{\sqrt{a_1^2-a_2^2}}*\sqrt{2*g*h_m*\frac{\rho_m}{\rho_w}}\right]*\rho_w}{\pi*d1*\mu_w}\text{..............eq.(12)}$$

d_1 = Pipe diameter = 0.0254 m

d_2 = Throat diameter = 0.016 m

a_1= Area of pipe $=\frac{\pi*d1^2}{4}=\frac{\pi*0.0254^2}{4}=5.06*10^{-4}m^2$

a_2 = Area of throat $=\frac{\pi*d2^2}{4}=\frac{\pi*0.016^2}{4}=$ $2.016*10^{-4}$ m^2

$$R_e=\frac{4*\left[\frac{5.067*10^{-4}*2.0106*10^{-4}}{\sqrt{(5.067*10^{-4})^2-(2.0106*10^{-4})^2}}*\sqrt{2*9.81*h_m*\frac{13.6}{1000}}\right]*1000}{\pi*0.0254*8.315*10^{-4}}$$

$$R_e=\frac{4*[2.189*10^{-4}*16.33*\sqrt{hm}]*1000}{6.635*10^{-5}}$$

$$R_e=21.5514*10^4*\sqrt{hm}$$

$$\sqrt{hm}=\frac{R_e}{21.55*10^4}m$$

For minimum Reynolds number $R_{e_{min}}$= 16846

$$h_m=\left(\frac{16846}{21.55*10^4}\right)^2=6.1108*10^{-3}\text{ m}$$

For maximum Reynolds number $R_{e_{max}}$ = 134775

$$h_m=\left(\frac{134775}{21.55*10^4}\right)^2=0.3911\text{ m}$$

Venturimeter is calibrated between R_e number 10000-10000

Deflections of mercury in differential manometer are:

- If R_e = 10000

$$\sqrt{hm}=\frac{R_e}{21.55*10^4}\text{ ....eq. (13)}$$

$$h_m=\left(\frac{R_e}{21.55*10^4}\right)^2=\left(\frac{10000}{21.55*10^4}\right)^2=2.1533*10^{-3}\text{ m}=2.1533\text{ mm}$$

- If R_e =12500

$$h_m=\left(\frac{R_e}{21.55*10^4}\right)^2=\left(\frac{12500}{21.55*10^4}\right)^2=3.364*10^{-3}\text{ m}=3.364\text{ mm}$$

- If R_e =15000

$$h_m=\left(\frac{R_e}{21.55*10^4}\right)^2=\left(\frac{15000}{21.55*10^4}\right)^2=4.845*10^{-3}\text{ m}=4.845\text{ mm}$$

- If R_e=17500

$$h_m=\left(\frac{R_e}{21.55*10^4}\right)^2=\left(\frac{17500}{21.55*10^4}\right)^2=6.594*10^{-3}\text{ m}=6.594\text{ mm}$$

Trial 1 :

Table No 1: Venturimeter Calibration

Reynolds number	Deflection in mm	Actual deflection in mm	Corresponding Re	Q actual	Q the.	cd
10000	2.36	2	9311.432	8.69E-05	1.54E-04	0.564
12500	3.604	4	13168.35	1.78E-04	2.18E-04	0.816
15000	5.19	5	14722.67	2.31E-04	2.44E-04	0.949
17500	7.06	7	17420.09	2.60E-04	2.88E-04	0.9
20000	9.226	9	19752.53	2.96E-04	3.27E-04	0.905
22500	11.67	12	22808.26	3.38E-04	3.77E-04	0.895
25000	14.41	14	24635.73	3.74E-04	4.08E-04	0.917
27500	17.44	17	27147.26	4.10E-04	4.49E-04	0.914
30000	20.76	21	30172.49	4.85E-04	4.99E-04	0.971
32500	24.36	24	32255.75	5.03E-04	5.34E-04	0.94
35000	28.35	27	34212.39	5.29E-04	5.66E-04	0.935
37500	32.43	29	35456.89	5.50E-04	5.86E-04	0.93
					Standard deviation	0.023917451
					Avg. Cd	0.9256
					% Error	2.583994234

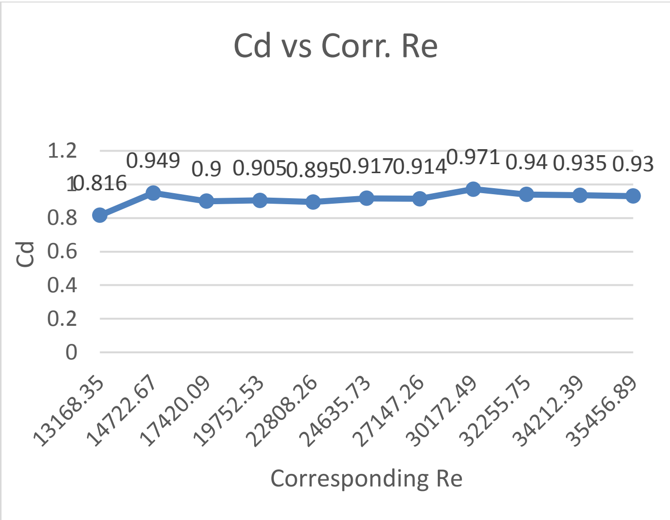

Fig.5.3: Graph showing Cd vs Re

The thermo couple used to measure jet temperature is calibrated. The calibration procedure is as explained below. Two junctions are formed by the K type thermocouple wire. One of the junctions (cold junction) is maintained at 0^0C b y dipping it in a test tube enclosed in a thermos flask whose lid is provided with a hole to insert the wire in to the flask. The test tube containing mercury and water is surrounded by ice and water in equilibrium.Thecoldjunctionismaintainedatthemercurywater interface.Thelidof the thermos flask is closed tightly for minimizing the heat transfer into the flask. The other Junction (hot junction) is dipped in a water bath. Standards are in contact with the water .Calibrated RTD, thermocouple and thermometer are chosen as standards and their average readings are used to calibrate the present thermocouple. A milli volt meter is connected between the two junctions to give the emf developed in the circuit.
The arrangement is as shown in Fig.5. Initially, water in the water bath is heated to the temperature of about95^OC (*i.e.*, the temperature more than the maximum temperature obtained during the experimentation).Then, the electrical power to the water bath is switched off and temperature of water is allowed to drop. During cooling, mill volt meter readings, temperature readings from the calibrated thermometer, RTD and the K type thermocouple are noted at every 5^0Cdecrease in thermometer reading

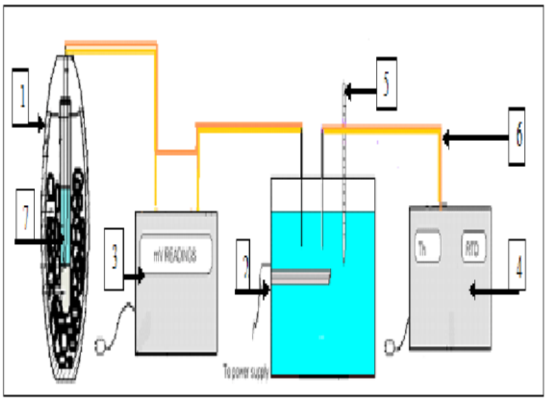

Fig.5.4: Thermocouple arrangement

1)Thermos flask 2)Water bath 3)Mill voltmeter 4)Tutor 5)Calibrated thermometer 6)K type thermocouple wire 7) Test tube Experimental set-up for calibration of thermocouple .A linear fit is obtained (Fig---)for the variation of emf with average temperature valuesfrom95^OCto25^OC .And the calibration equation is T(^{0}C) = 23.188*v+3.8439

Table No 3: Calibration of Thermocouple

Temperture	voltmeter reading
25.6	0.94
30.1	1.13
34.6	1.33
39.8	1.55
44.9	1.77
49.8	1.98
54.7	2.19
59.7	2.41
64.6	2.62
69.7	2.84
75	3.07
79.8	3.28
84.6	3.48
89.7	3.7
94.7	3.92

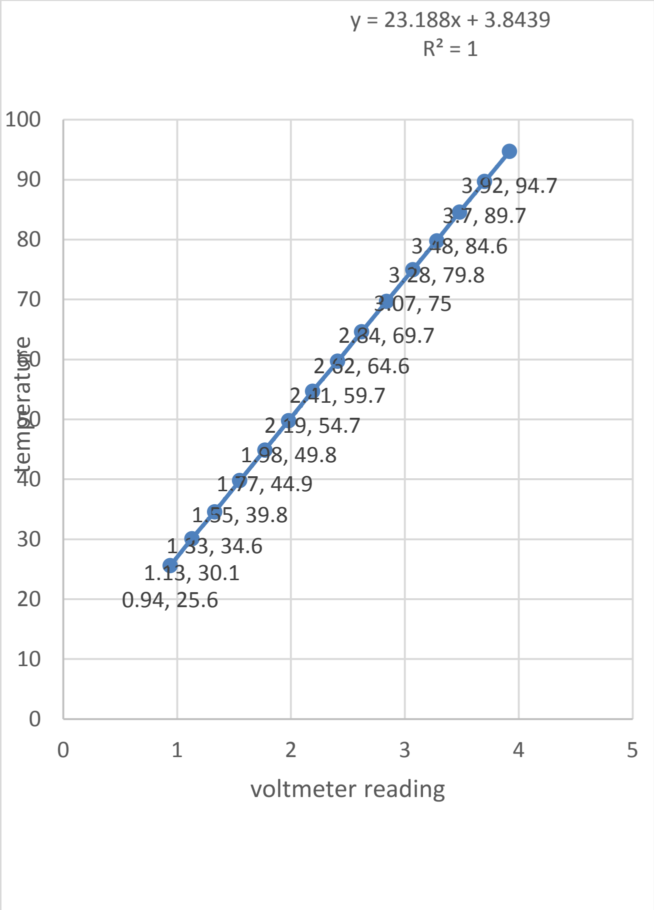

Fig.5.5: Graph showing Temperature vs. mili voltmeter reading.

Magnification Factor

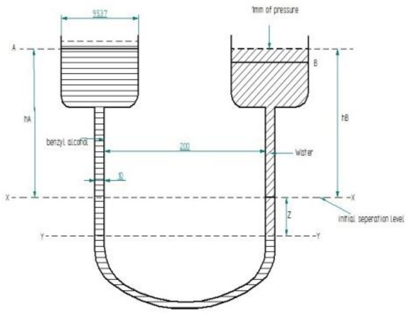

Fig.5.6: Magnification Factor

Diameter of each bulb = D =95.37mm
Diameter of the limb = d =10mm
Density of Benzyl Alcohol = 1045 $\frac{Kg}{m^3}$
Density of Water = 1000 $\frac{Kg}{m^3}$
Cross sectional area of the Bulb =$\frac{\pi}{4}D^2 = \frac{\pi}{4}(0.09537)^2$ = 7.143x10^-3 m^2 …eq. (14)
Cross sectional area of the limb =$\frac{\pi}{4}d^2 = \frac{\pi}{4}(0.01)^2$ = 7.854x10^-3 m^2 ….eq. (15)
Let,
X-X be the initial separation level
H_b= height of the benzyl Alcohol above X-X
H_w= Height of the water above X-X

Pressure above X-X in the left limb = 1045 x 9.81 x $H_b \frac{N}{m^2}$ ………..eq.(16)

Pressure above X-X in the right limb = 1000 x 9.81 x $H_w \frac{N}{m^2}$ ……..eq. (17)

Equating the two pressures, we get
1045 x 9.81 x H_b= 1000 x 9.81 x Hw
H_w = 1.045 H_b(1)……eq.(18)
When pressure head over the surface in C increased by 1mm of water, let the separation level falls by an amount Z. Then Y-Y becomes the new separation level.
Now fall in surface level of C multiplied by Cross sectional area of bulb C must be equal to the fall in separation level multiplied by cross sectional area of the limb.
Therefore,

$$= \frac{\text{Fall in seperation level} * a}{A}$$

$$= \frac{Z \text{ x } 7.854\text{x}10\text{^}{-3}}{7.143\text{x}10\text{^}{-3}}$$

$$= \frac{Z}{90.95}$$

Also,

Rise in surface level B=$\frac{Z}{90.95}$.

The pressure of 1mm of water = ρ g h = 1000 x 9.81 x 0.001 = 9.81 $\frac{N}{m^2}$

Pressure above Y Y in the left limb = 1000 x 9.81$\left[Z + Hb + \frac{Z}{90.95}\right]$ …..eq.(19)

Pressure above Y Y in the right limb = 1000 x 9.81$\left[Z + Hw - \frac{Z}{90.95}\right]$ + 9.81……eq. (20)

Equating the two pressures, we get

1000 x 9.81$\left[Z + Hb + \frac{Z}{90.95}\right]$ = 1000 x 9.81$\left[Z + Hw - \frac{Z}{90.95}\right]$ + 9.81 ……eq. (21)

Solving and substituting result 1, we get
Z = 14.59mm

6. EXPERIMENTAL SETUP AND METHODOLOGY

The schematic lay-out of the experimental set-up is shown in Fig. ----.The experimental set up consists of Air blower of 600 watts capacity (Make- AEG GM 600E), 6 speed having minimum and maximum flow rate 0.36 m^3/min and 2.8 m^3/min. The venturimeter is designed for this flow range and throat and inlet diameters are 16 mm and 25.4 mm. The venturimeter is calibrated with water for the Reynolds No. 10000-100000. C_d of venturimeteris found to be 0.92355±2%
The flow rate is controlled by flow control valves, the Reynolds number is set by adjusting the flow rate with the calibrated venturimeter. The temperature of the air is measured by using k-type thermocouple placed near the nozzle exit. It is calibrated with RTD and the relation between temperature and mv obtained is t=23.188v+3.8439 with R^2 = 1.
In addition, all experiments were performed under a steady state condition so that accurate temperature data could be obtained

ISSN: 2278-0181

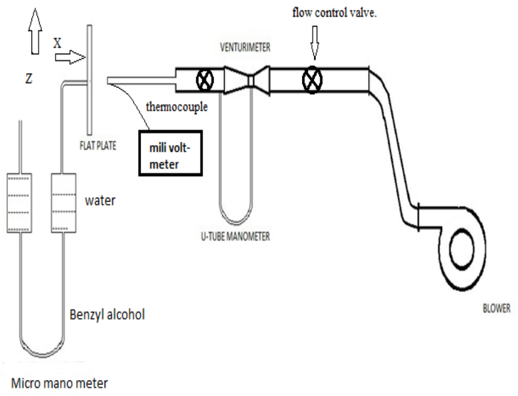

Fig.5.6: Schematic diagram of experimental setup

Acrylic cylinder of inner diameter 50mm and thickness 5mm is used as flat surface and static pressure difference is measured by double bulb, two fluid micro-manometer using Benzyl alcohol and water as manometer fluids, with magnification factor 14.59.

7. EXPERIMENTATION

The experiment carried out for different (Z/D) ratios. The (Z/D) ratio ranging from 0.5 to 4.5

Observation table for (Z/D)=0.5

Table No:7.1

Z/d=0.5 for Reynolds 14867.42936

	milivoltmeter reading 'mV'	longitudinal distance in 'mm'	static pressure difference in	presurre in 'pa' Δp	Discharge Q	velocity of air at nozzle 'V_j'	temperature of air at nozzle 't'	density 'ρ'	Absolute viscocity 'μ'	Reynolds number of flow at nozzle 'Re'	cp	x/d
12	1.17	0	26	255.06	0.00290293	15.38990842	30.97386	1.16410456	1.86777E-05	14867.42936	1.850155749	0
12	1.17	1	25.7	252.117	0.00290293	15.38990842	30.97386	1.16410456	1.86777E-05	14867.42936	1.828807798	0.06451
12	1.18	2	24.4	239.364	0.00290293	15.38990842	31.20574	1.16317704	1.86891E-05	14846.55195	1.73768454	0.129
12	1.19	3	22.54	221.1174	0.00290293	15.38990842	31.43762	1.16224952	1.87004E-05	14825.69992	1.606502731	0.1935
12	1.19	4	20.21	198.2601	0.00290293	15.38990842	31.43762	1.16224952	1.87004E-05	14825.69992	1.440435679	0.258
12	1.19	5	18.16	178.1496	0.00290293	15.38990842	31.43762	1.16224952	1.87004E-05	14825.69992	1.294325182	0.3225
12	1.2	6	15.62	153.2322	0.00290293	15.38990842	31.6695	1.161322	1.87118E-05	14804.87321	1.114179871	0.387
12	1.2	7	12.8	125.568	0.00290293	15.38990842	31.6695	1.161322	1.87118E-05	14804.87321	0.913028319	0.4516
12	1.2	8	10.14	99.4734	0.00290293	15.38990842	31.6695	1.161322	1.87118E-05	14804.87321	0.723289622	0.5161
12	1.21	9	7.88	77.3028	0.00290293	15.38990842	31.90138	1.16039448	1.87232E-05	14784.07178	0.56253234	0.5806
12	1.21	10	5.89	57.7809	0.00290293	15.38990842	31.90138	1.16039448	1.87232E-05	14784.07178	0.420471508	0.6451
12	1.21	11	4.31	42.2811	0.00290293	15.38990842	31.90138	1.16039448	1.87232E-05	14784.07178	0.307679491	0.7096
12	1.21	12	3.24	31.7844	0.00290293	15.38990842	31.90138	1.16039448	1.87232E-05	14784.07178	0.231295023	0.7741
12	1.21	13	2.67	26.1927	0.00290293	15.38990842	31.90138	1.16039448	1.87232E-05	14784.07178	0.190604232	0.8387
12	1.21	14	2.19	21.4839	0.00290293	15.38990842	31.90138	1.16039448	1.87232E-05	14784.07178	0.156338303	0.9032

8. RESULTS AND DISCUSSION

An experiment is conducted on the concave flat surface to determine coefficient of static pressure (C_p=Δp/0.5ρAV_j^2) by impinging air jet by the circular straight nozzle at steady state. Experiments are conducted for different Reynolds number ranging from 12000 to 47000 for various circumferential angles (ϴ=0-35°), longitudinal distance from point of impingement of jet (X=0 -14 mm), and distance between target plate and nozzle (Z=7.75-124 mm). However the dimensionless distance x/d and Z/d are considered for the analysis, where d=15.5mm, is the diameter of circular straight nozzle.

From the graph of C_p v ϴ, and C_p v X/D, for varios Reynolds number, it is observed that, coefficient of static pressure (C_p) is independent of Reynolds number as the curves overlaps to each other and same trend is observed for all Z/D ratio. Hence further analysis is carried out for one representative Reynolds Number(Re=30000

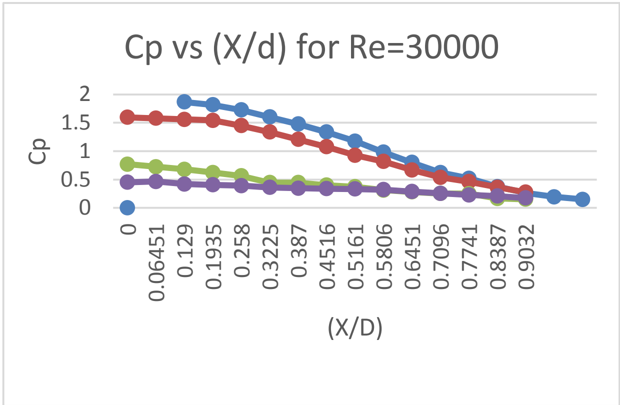

Fig.8.1: Influence of longitudinal distance from point of impingement(X/D) on C_P for various Z/D ratio for Re=30000

1From the graph of $C_p$vs x/d graph, the values of C_p is higher for lower x/d ratio. They decrease gradually up to X/D=0.13 and then appreciable decrease of C_p is observed for further increase in X/D ratio. The atmospheric pressure is reached on the concave surface at X/D ≈1. This indicates that atmospheric condition is reached on the concave surface due to impingement of jet at a longitudinal distance equal to the diameter of jet

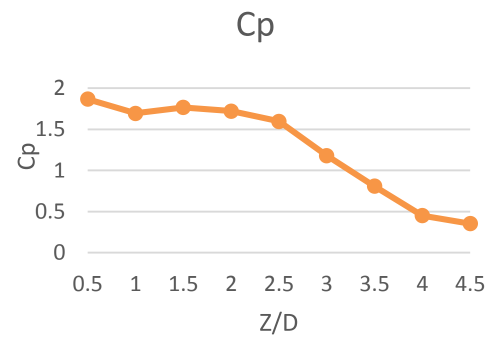

Fig.8.2: Influence of longitudinal distance from point of impingement(X/D) on C_P for various Z/D ratio

From the graph of C_{P0} (Stagnation pressure co-efficient) v Z/D ratio, C_{P0} decreases as Z/D ratio increases up to 1. The value of C_{P0} remains more or lessuniform in the range of Z/D=1 to3. This may be because of target plate located within the potential core of free jet. Then the appreciable decrease ofC_{P0} is observed for further increase of Z/D ratio. As the distance from the nozzle increases the velocity goes on decreasing monotonically due to spreading of jet.

9. CONCLUSION

The effect of Circumferential angle of concave flat surface *ϴ* from point of impingement of air jet, the longitudinal distance X/D and distance of target surface form nozzle Z/D on Coefficient of static pressure C_p is experimentally investigated for different Reynolds number of flow at steady state. The followings are the main conclusions that may be drawn from this study.

- The static pressure distribution on the target surface due to impingement of jet is independent of Reynolds Number of flow.

- The values of static pressure Coefficient C_{p0} at stagnation points are higher due to higher centerline velocities at stagnation.

- The values of static pressure Coefficient C_p on the concave flat surface are almost uniform up to curvature angle of 5°, and decrease appreciably for higher values of ϴ.

- The values of static pressure Coefficient C_p on the concave flat surface are higher for lower X/d ratio, they decrease gradually up to X/D=0.13, and appreciable decrease of C_p is observed for further increase of X/D ratio.

The potential core of free jet is observed for the Z/D ratio between 1and 3. The velocity decay is minimum for this range of Z.

10. REFERENCES

[1] Vantreurn K.W "Impingement flow heat transfer measurements of turbine blades using a jet array", Ph D Thesis, University of Oxford, Trinity Term (1994).
[2] Han J.C Dutta Ekkad S.V "Gas turbines heat transfer and cooling technology", Taylor and Francis,(2000) pp.2.
[3] Livingood J.N.B and Hrycak P 1970 "Impingement heat transfer from turbulent air jets to flat plates.-A Literature Survey", NASA Technical Memorandum NASA TM X-2778.
[4] Martin H 1977 "Heat and mass transfer between impinging gas jets and solid surfaces '' Adv heat transfer 13, pp1-60.
[5] Jambunathan K., Lai E., Moss M.A., Button B.L., 1992 "A Review of Heat Transfer Data for Single Circular Jet Impingement'', Int.J.Heat Fluid Flow, 13, pp 106-115
[6] Viskanta R., 1993, "Heat Transfer and Fluid Science, 6, pp 111-134.
[7]Chupp R.E.,Helms H.E.,Mc Fadden P.W., Brown T.R.,1969, "Evaluation of Internal Heat –transfer coefficient for impingement-cooled Turbine Air foils'' ,J Aircraft,6(3),pp 203-208.
[8] Jusionis V.J., 1970, "Heat Transfer from Impinging Gas Jets on an Enclosed Concave Surfaces' ' ;J. Aircraft, Jan-Feb, pp 87-88.
[9] Metzger D.E., Yamashita T., Jenkins C.W., 1969, "Impinging Cooling of Concave Surfaces with line of circular Air Jets'', J Engg.for power, July,pp 149-158.
[10] Metzger D.E.Baltzer R.T.,Jenkins C.W.,1972, "Impingement Cooling Performance in Gas Turbine Airfoils including Effects of leading Edge Sharpness", J. Engg. For Power, July, pp 219-225.
[11] Dyban Y.P.and Mazur A.I., 1970, Heat-transfer-Soviet Research, 2(3), pp 15-20.
[12] Taslim, M.E., Pan Y and spring S.D., 2001, "An Experimental study of Impingement on Roughened Airfoil Leading-Edge walls with film Holes" ASME J.Turbomach., 123, October, pp, 766-773.
[13] Taslim, M.E., Setayeshgar, L., and spring S.D., 2001. "An Experimental evaluation of advanced leading Edge Impingement Cooling Concepts," ASME J.Turbomach., 123, 2, pp.147-153
[14] Taslim, M.E., Pan Y.and Bakhtari K., 2002, "Experimental Racetrack Shaped Jet Impingement on a Roughened Leading-Edge Wall with Film Holes,". Paper No. GT 2002-30477.
[15] Taslim, M.E., Bakhtari K., and Liu,H.,2003, "Experimental and Numerical Investigation of Impingement on a Rib- Roughened Leading-Wall," ASME J.Turbomach.,125,pp.682-691.
[16] Taslim, M.E., and Khanicheh , A.,2006 "Experimental and Numerical Study of Impingement on an Airfoil Leading-Edge with and without Showerhead and Gill Film Holes," ASME J. Turbomach.,128,2,pp.310-320.
[17] Taslim, M.E.,and Bethka,D.,2009, "Experimental and Numerical in an Airfoil Leading-Edge Cooling channel with cross-flow'', ASME J.Turbomach.131,1,PP.011021-1-7
[18] Iacovides H.,Kounadis D.,Launder B.E.,Li J.and Xu Z., 2005, "Experimental Study of the Flow and Thermal Development of a Row of Cooling Jets Impinging on a Row Rotating Concave Surfaces", ASME J. Turbomach.,127,1,pp.222-229
[19] Craft T.J, Iacovides H., and Mostafa N.A.,2008, " Modeling of three-dimensional jet array impingement and heat transfer on a concave surfaces",Int.J. Heat transfer on a concave surfaces", Int.J.Heat Fluid flow, 29, pp 687-702.
[20] Fenot M.,Doringnac E., Vullierme J-J.,2008, "An Experimental study on hot round jets impinging a concave surface",Int. J .Heat Fluid Flow, doi:10.1016/j.ij heat fluid flow.2008.03.015.
[21] Tabak off , W and Clevenger ,W.,1972 "Gas Turbine Blade Heat Transfer Augmentation by impingement of Air Jets Having Various Configurations", J.Engg.for power,94,pp 51-60
[22] Flors chuetz L.W., Metzger D.E., and Truman C.R., 1981, "Jet Array Impingement with cross flow-Correlation of Stream wise Resolved Flow and Heat Transfer Distributions", NASA Contractor Report 3373.
[23] Choi,M.,Yoo,H.S.,Yang,J.S.,and Sohn,D.K.,2000 "Measurements of Impinging Jet Flow and Heat Transfer on a Semi-Circular Concave Surface",Int.J. Heat Mass Transfer, 43, pp1811-1822.
[24] Ramakumar .V.N.and Prasad B.V.S.S.S., 2006 "Experimental and Computational Study of Multiple Circular Jets Impinging on a Concave Surface" Proceedings of 33rd National and 3rd International Conferences on Fluid Mechanics and Fluid Power, IT Bombay, India.
[25] Ramakumar B.V.N.and Prasad B.V.S.S.S., 2007, "Computational Flow and Heat Transfer of a Row of Circular Jets Impinging on a concave Surface", Heat Mass Transfer (Springer Verlag),DOI 10.1007/s00231-007-0274-3
[26] Bunker R.S., "Gas turbine heat transfer: Ten remaining hot gas path challenges", J.Turbomachinery, 129(2007) 193-201.
[27] Lytle D.and Webb B.W., "Air Jet Impingement Heat Transfer at low Nozzle Plate Spacings", Int.J.Heat Mass Transfer, 37(1994) 1687-1697.
[28] Moffat R.J., "Describing the Uncertainties in experimental results", Experimental Thermal and Fluid Science, 1(1988) 3-17.
[29] K L Kumar, Engineering Fluid Mechanics, 81-219-0100-6, 2007 edition.